

Experimental Determination of the Rotational Constants of High-Lying Vibrational Levels of Ultracold Cs_2 in the 0_g^- Purely Long-Range State

Jie Ma,^{*,†} Jizhou Wu,[†] Gang Chen,[†] Qunchao Fan,[‡] Hao Feng,[‡] Xingcan Dai,[§] Weiguo Sun,^{‡,||} Liantuan Xiao,[†] and Suotang Jia[†]

[†]State Key Laboratory of Quantum Optics and Quantum Optics Devices, Laser Spectroscopy Laboratory, Shanxi University, Taiyuan 030006, China

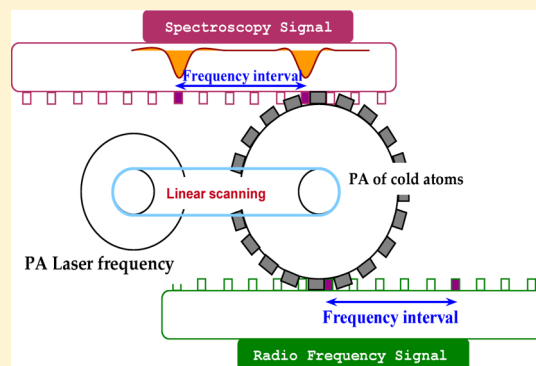
[‡]School of Physics and Chemistry, Research Center for Advanced Computation, Xihua University, Chengdu, Sichuan 610039, China

[§]State Key Laboratory for Low-Dimensional Quantum Physics, Department of Physics, Tsinghua University, Beijing 100084, China

^{||}Institute of Atomic and Molecular Physics, Sichuan University, Chengdu, Sichuan 610065, China

S Supporting Information

ABSTRACT: We report on a quantitative experimental determination of the rotational constants for the high-lying vibrational levels of the ultracold pure long-range Cesium molecules formed via photoassociation. The scheme relies on a precise reference of frequency difference in a double photoassociation spectroscopy, which is induced by two laser beams based on an acoustic-optical modulator. The rotational constants are obtained by fitting a nonrigid rotor model into the frequency intervals of the neighboring rotational levels deduced from the reference.



SECTION: Spectroscopy, Photochemistry, and Excited States

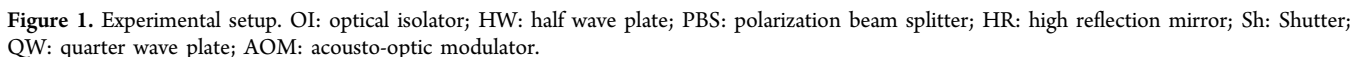
Research on ultracold molecules¹ has received much attention in the past decade due to important advances and potentially new applications in several domains such as superchemistry,² control of chemical reactions,³ and physical chemistry.⁴ Many methods to produce ultracold molecules have been proposed.⁵ Photoassociation (PA) of ultracold atoms is one of the most efficient techniques.⁶ PA provides a unique opportunity to obtain information on the molecular long-range and even purely long-range⁷ (PLR) state. In addition, PA has been used extensively to make precise measurements of the high-lying vibrational levels that are essential to determine the molecular parameters near dissociation limits and often difficult to access with traditional bound-bound molecular spectroscopy.

Numerous experimental studies have been reported about the PLR Cesium molecule (Cs_2) formed by PA, for instance, resonant four-body interaction in cold Cesium Rydberg atoms,⁸ absolute frequency stabilization to Cesium atom molecular hyperfine transitions,⁹ and precise measurement of Cesium atomic triplet state scattering length.¹⁰ Very recently, the vibrational spectral data of Cs_2 0_g^- PLR state below dissociation limit ($6S_{1/2} + 6P_{3/2}$) had extended down to the lowest level ($v = 0$) by using trap-loss detection.¹¹ Because PA spectra generate rich rotational data, a reasonable investigation is

required to precisely determinate the rotational constants of the PLR molecules, and the rotational constants are crucial in predicting the unexplored levels and obtaining the precise potential energy curve.¹² Recently, some efforts have been made to obtain the rotational constants of the low-lying vibrational levels in the Cs_2 0_g^- PLR state.¹³ However, the rotational constants of the high-lying vibrational levels, which are important for precisely obtaining the near-dissociation part of potential energy curves, is difficult to determine by the conventional direct measuring method of using a high-resolution wavelength meter because of the small frequency interval of the neighboring rotational levels.¹⁴ An available method is to employ a Fabry–Perot reference cavity to monitor the changes of the relative frequency. However, the rotational constants of Cs_2 high-lying vibrational states have not been obtained using this scheme, the sensitivity of which is not sufficiently high for measuring the small frequency intervals. In particular, the measuring accuracy of the Fabry–Perot reference cavity is greatly reduced by the low frequency $1/f$ noise, which results from the long scanning time in PA experiments.

Received: August 19, 2013

Accepted: October 10, 2013



PA is induced by a cw widely tunable Ti:sapphire laser system (Coherent MBR-110, ~ 1 W with line-width of 0.1 MHz). The long-time frequency drift of Ti: sapphire laser system is less than 500 kHz by locking it to its self-reference

In order to determine the rotational constants of high-lying vibrational levels, we directly measure the frequency interval of the neighboring rotational levels by employing a precise reference of frequency difference that is based on a “double PA spectrum” with high resolution. The double PA spectrum is obtained through alternately illuminating the cold atomic sample by two laser beams (laser I and laser II) with a fixed frequency interval and the same laser intensity. The two beams are controlled by two shutters (Sh1, and 2); thus rotational levels induced by the different beams are recorded in the

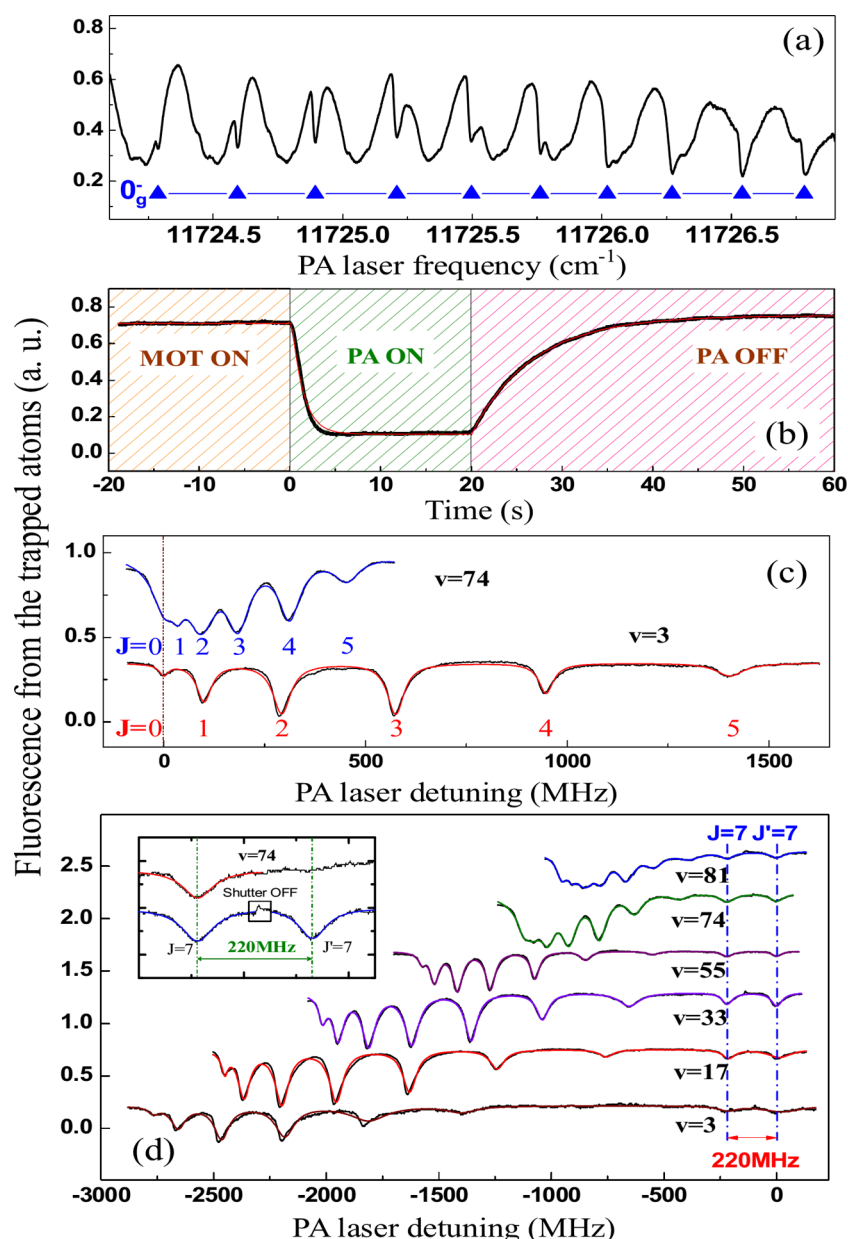


Figure 2. (a) A vibrational spectrum for the high-lying vibrational levels of the Cs_2 0_g^- PLR state is recorded in the range of -5.5 cm^{-1} to 7.9 cm^{-1} below the dissociation limit ($6S_{1/2} + 6P_{3/2}$). (b) Time evolution of the fluorescence with turning PA laser on and off is shown when MOT is working. (c) The high-resolution PA spectra of $v = 74$ and $v = 3$ vibrational levels of the Cs_2 0_g^- PLR state induced by laser I are shown. (d) Six typical spectra with the reference of frequency difference are provided for vibrational levels $v = 81, 74, 55, 33, 17$, and 3 . The intensities of the laser I and II are 40 W/cm^2 and keep unchanged. The colorful curves are the multipeak Lorentzian fitting results. The colorful curves are fitted in a Lorentzian multipeak function.

frequency spectrum, namely “double photoassociation spectroscopy”. As shown in Figure 1, the matching lasers (I and II) are introduced using an acousto-optic modulator (AOM) (MT110-B50A1-IR, AA Optoelectronic). The AOM diffracts the incident PA laser beam into different orders and shifts its frequency with the acoustic frequency, which can be altered by the offset potentiometer. The frequency interval is set according to the resonance peak interval between the rotational progressions. For the high-lying vibrational levels of the Cs_2 0_g^- PLR state, the peak interval between rotational levels is about 30–200 MHz. Thus, we set the central frequency of the AOM on 110 MHz and apply a double pass scheme to obtain the frequency interval of 220 MHz between laser I and II as the fixed frequency interval to avoid disturbance coming from the

neighboring rotational progressions. We adjust the half wave plates (HW_1) and polarization beam splitter (PBS_1) to make sure that the intensities of the laser I and II are the same, 200 mW, in order to avoid the frequency shift induced by PA laser intensity.²¹

A typical PA vibrational spectrum, which specifies the high-lying vibrational levels of the Cs_2 0_g^- PLR state, is acquired when the atomic sample is illuminated only by beam I with an intensity of 40 W/cm^2 , as shown in Figure 2a. The PA laser is rapidly scanned at a rate of 300 MHz/s. The continuity and linearity of the frequency scans are monitored by the wavelength meter. Using the spectral features and ionization spectroscopy data,²² the vibrational progressions can be assigned to three long-range Hund’s case (c) states, the $0_u^+, 1_g$

long-range states and the 0_g^- PLR states. Here we focus on just the 0_g^- PLR state, whose vibrational states of $\nu = 73\text{--}82$ are indicated by the blue triangles.

Figure 2b shows the time evolution of the fluorescence with turning PA laser on and off, which give characteristic times of $t_{\text{on}} = 1.26\text{ s}$ and $t_{\text{off}} = 6.80\text{ s}$ by exponential fits, respectively. Thus, the PA laser scanning rate should be smaller in order to obtain high-resolution rotational spectroscopy. The scan rate of the PA laser is 5 MHz/s in these experiments. Figure 2c shows the measured high resolution PA spectra induced only by laser I, which are related to the $\nu = 74$ and $\nu = 3$ vibrational levels of the Cs_2 0_g^- PLR state. Note that the resolved rotational structure ($J = 0 \sim 5$) is clearly seen. Compared with the frequency intervals of the neighboring rotational levels of the low-lying vibrational states (such as $\nu = 3$), the frequency intervals of the high-lying vibrational states (such as $\nu = 74$) is rather small.

As the rotational progressions are often difficult to distinguish, levels above $\nu = 74$ have been arbitrarily labeled by $J = 2$.¹⁴ In our experiments, the PA spectra for the high-lying vibrational states ($\nu = 73\text{--}82$) of the Cs_2 0_g^- PLR state below dissociation limit ($6S_{1/2} + 6P_{3/2}$) with the resolved rotational structure have been directly obtained based on a robust modulation spectral technique.²³ In order to precisely measure the frequency interval of the neighboring rotational levels, the double PA spectroscopy has been employed as a precise reference of frequency difference. Laser II is blocked by the shutter 2 in the beginning and laser I interacts with ultracold atoms during the defined scanning range. As the spectral signal of $J = 7$ is scanned, laser I is instantaneously obstructed by turning shutter 1 on. Simultaneously, by turning the shutter 2 off, the laser II can interact with the atomic cloud in succession. Then the $J' = 7$ resonance of the same vibrational state induced by laser II only is presented in Figure 2d. Figure 2d shows six typical spectra for vibrational quantum number $\nu = 81, 74, 55, 33, 17$, and 3 , whose detunings are $\sim 6\text{ cm}^{-1}$, $\sim 8\text{ cm}^{-1}$, $\sim 16\text{ cm}^{-1}$, $\sim 33\text{ cm}^{-1}$, $\sim 51\text{ cm}^{-1}$, and $\sim 72\text{ cm}^{-1}$ below the dissociation limit ($6S_{1/2} + 6P_{3/2}$), respectively. The time for switching the two shutters is shorter than the loading time ($\sim 1\text{ s}$); thus the resonance peaks are clearly demonstrated without affecting each other, as shown in the inset of Figure 2d. When the intensities of the two lasers are the same (for example, 40 W/cm^2 in our experiment), the PA spectra induced separately by them have the same loss ratio (i.e., the loss to initial atomic fluorescence amplitude ratio) and line-width broadening. Thus, the intensity induced frequency shift induced by laser II (in this case, $J = 7$) is equal to that induced by laser I ($J' = 7$). Consequently, the frequency interval between the two peak positions of $J = 7$ and $J' = 7$ is exactly the fixed frequency interval of the two lasers, 220.0 MHz , which provides a precise reference of frequency difference. The value of frequency difference can be set through the AOM, whose accuracy is measured in kilohertz. Based on the precise reference, the value of the small rotational frequency interval can be directly obtained on the condition that the PA laser is linearly scanning.

In order to obtain the rotational constants for the high-lying vibrational levels, we investigated the dependence of rotational frequency interval ($\Delta\nu$) on rotational quantum progression ($J = 0\text{--}6$) for different vibrational levels. Figure 3(a) shows the nonlinear relationship between $\Delta\nu$ and J for the vibrational levels ($\nu = 55, 74$, and 81). The main reason for the nonlinearity is that the long-range interaction between the two constituent atoms of the PLR molecules is rather weak

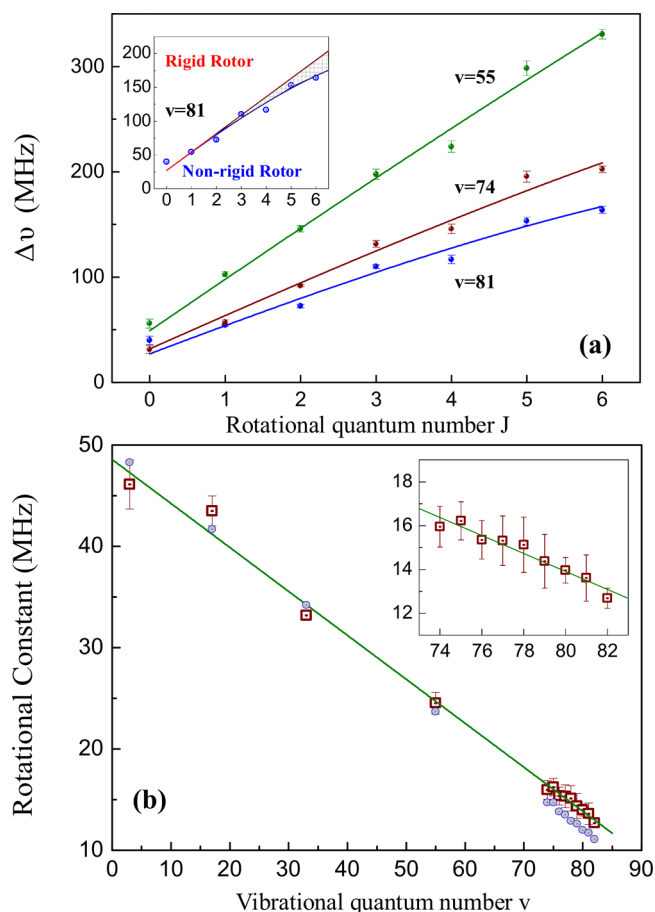


Figure 3. (a) Dependence of the frequency intervals $\Delta\nu$ on J for $\nu = 81, 74$, and 55 of the Cs_2 0_g^- PLR state. The symbols represent experimental data, while the lines are the fits to the nonlinear nonrigid rotation model. The square of the correlation coefficient (R^2) in the fit process is up to 0.95 for each ν . The inset shows the difference between the rigid and nonrigid rotation models. (b) Dependence of the obtained B values (brown squares) on ν of Cs_2 0_g^- PLR state. The inset shows the determined rotational constant for the high-lying vibrational levels. The blue circles represent the corresponding theoretical values of the rotational constants for different vibrational states listed in ref 14.

comparing with the ordinary chemical bond. The color curves are the fits plotted in accordance with a nonrigid rotor model.²⁴ The rotational frequency interval is described as $\Delta\nu = 2B(J + 1) - 4D(J + 1)^3$, where B is the rotational constant and D is the centrifugal distortion constant (also listed in the Supporting Information). In order to test the appropriateness of this nonlinear model, we compare the nonrigid and rigid rotor model, as shown in the inset of Figure 3a. As a result, we obtain a series of the rotational constants of different vibrational levels ($\nu = 3\text{--}82$) of the Cs_2 0_g^- PLR state.

Figure 3b shows the rotational constants as a function of vibrational quantum number ν . In particular, the rotational constants of the high-lying vibrational levels ($\nu = 74\text{--}82$) are shown in the inset of Figure 3b. The uncertainty is mainly due to a possible statistical error in the process of fitting as well as the error in the determination of the resonant line position. It is valuable to find that the rotational constants decrease gradually with increasing ν in the case of high-lying vibrational levels and reach ultimately zero at the range of dissociation limit, and it can be understood by considering the molecular internuclear

separation as described in ref 13. In addition, the rotational constants of the high-lying vibrational levels ($v = 74\text{--}82$) are consistent with those of the low-lying vibrational levels. The green curve is the linear regression result. The square of coefficient of correlation is 0.995, and the regression coefficient is -0.42 MHz. For comparison, we also present in Figure 3b the corresponding theoretical values of the rotational constants for different vibrational states listed in ref 14. The current experimental results demonstrate a similar trend with the theoretical values (the regression coefficient is -0.47 MHz). The experimental results and the theoretical calculations show a good level of agreement.

In conclusion, a double PA spectroscopy technique has been proposed for providing a precise frequency reference to experimentally determine the rotational constants of high-lying vibrational levels of the molecular PLR state. A linear dependence of the rotational constants on the vibrational quantum number is found. The proposed technique allows one to reach all the data of available experimental ro-vibrational levels below the dissociation limit. Nevertheless, at the present stage of the experiment, the interpretation of the results remains limited, due to not considering the perturbation effect that stems from the mixing with the triplet sigma ungerade levels. The pure long-range 0_g^- states are Hund's case (c) states that result from a mixing between the $^3\Sigma_g^+(6s + 6p)$ and $^3\Pi_g(6s + 6p)$ Hund's case (a) electronic states.^{25,26} Although perturbations between the 0_g^- states below the $(6S + 6P_{3/2})$ asymptote are much less pronounced than those in the $0_u^+(6S + 6P_{1/2})$ state,²⁶ which has been well utilized in production of ultracold molecules into deeply bound $X^1\Sigma_g^+$ ground-state levels,²⁷ more elaborate calculations of the mixing terms are probably needed. Also, the good agreement between the theoretical and experimental values of the rotational constants of high-lying vibrational levels is evidence in favor of the present analysis. Our scheme has several advantages. First, the rotational constants of the high-lying vibrational levels of Cesium molecular PLR states have been directly measured for the first time. Furthermore, a high-quality cavity, which is rather expensive and difficult to adjust, is not required. Finally, the simple and robust scheme can be adapted to a number of other PLR molecular species.

■ ASSOCIATED CONTENT

Supporting Information

Rotational constants for different vibrational states. This material is available free of charge via the Internet at <http://pubs.acs.org>.

■ AUTHOR INFORMATION

Corresponding Author

*E-mail: mj@sxu.edu.cn.

Notes

The authors declare no competing financial interest.

■ ACKNOWLEDGMENTS

This research is sponsored by the 973 Programs (No. 2012CB921603 and No. 2013CB922000), the 863 Program (No. 2011AA010801), the International Science and Technology Cooperation Program of China (No. 2011DFA12490), NSF of China (No. 61008012 and No. 10934004), the NSFC Project for Excellent Research Team (No. 61121064), and the

Specialized Research Fund for the Doctoral Program of Higher Education (No. 20101401120004).

■ REFERENCES

- (1) Dulieu, O.; Raoult, M.; Tiemann, E. Cold Molecules: A Chemistry Kitchen for Physicists? *J. Phys. B: At. Mol. Opt. Phys.* **2012**, *39*, E01.
- (2) Heinzen, D. J.; Wynar, R.; Drummond, P. D.; Kheruntsyan, K. V. Superchemistry: Dynamics of Coupled Atomic and Molecular Bose-Einstein Condensates. *Phys. Rev. Lett.* **2000**, *84*, 5029–5033.
- (3) Ospelkaus, S.; Ni, K. K.; Wang, D.; Miranda, M. H. G.; Neyenhuis, B.; Quémener, G.; Julienne, P. S.; Bohn, J. L.; Jin, D. S.; Ye, J. Quantum-State Controlled Chemical Reactions of Ultracold Potassium-Rubidium Molecules. *Science* **2010**, *327*, 853–857.
- (4) Yang, Y.; Liu, X.; Zhao, Y.; Xiao, L.; Jia, S. Rovibrational Dynamics of RbCs on its Lowest $^1\Sigma^+$ Potential Curves Calculated by Coupled Cluster Method with All-Electron Basis Set. *J. Phys. Chem. A* **2012**, *116*, 11101–11106.
- (5) Schnell, M.; Meijer, G. Cold Molecules: Preparation, Applications, and Challenges. *Angew. Chem., Int. Ed.* **2009**, *48*, 6010–6031.
- (6) Jones, K. M.; Tiesinga, E.; Lett, P. D.; Julienne, P. S. Ultracold Photoassociation Spectroscopy: Long-range Molecules and Atomic Scattering. *Rev. Mod. Phys.* **2006**, *78*, 483–535.
- (7) Stwalley, W. C.; Uang, Y.; Pichler, G. Pure Long-Range Molecules. *Phys. Rev. Lett.* **1978**, *41*, 1164–1167.
- (8) Gurian, J. H.; Cheinet, P.; Huillery, P.; Fioretti, A.; Zhao, J.; Gould, P. L.; Comparat, D.; Pillet, P. Observation of a Resonant Four-Body Interaction in Cold Cesium Rydberg Atoms. *Phys. Rev. Lett.* **2012**, *108*, 023005.
- (9) Ma, J.; Wang, L. R.; Zhao, Y. T.; Xiao, L. T.; Jia, S. T. Absolute Frequency Stabilization of a Diode Laser to Cesium Atom-Molecular Hyperfine Transitions via Modulating Molecules. *Appl. Phys. Lett.* **2007**, *91*, 161101.
- (10) Drag, C.; Laburthe, T. B.; T'Jampens, B.; Comparat, D.; Allegrini, M.; Crubellier, A.; Pillet, P. Photoassociative Spectroscopy as a Self-Sufficient Tool for the Determination of the Cs Triplet Scattering Length. *Phys. Rev. Lett.* **2000**, *85*, 1408–1411.
- (11) Zhang, Y. C.; Ma, J.; Wu, J. Z.; Wang, L. R.; Xiao, L. T.; Jia, S. T. Experimental Observation of the Lowest Levels in the Photoassociation Spectroscopy of the 0_g^- Purely-Long-Range State of Cs_2 . *Phys. Rev. A* **2013**, *87*, 030503(R).
- (12) Amiot, C.; Dulieu, O.; Gutterres, R. F.; Masnou-Seeuws, F. Determination of the Cs_2 $0_g^-(P_{3/2})$ Potential Curve and of Cs $6P_{1/2, 3/2}$ Atomic Radiative Lifetimes from Photoassociation Spectroscopy. *Phys. Rev. A* **2002**, *66*, 052506.
- (13) Ma, J.; Wu, J. Z.; Zhao, Y. T.; Xiao, L. T.; Jia, S. T. Determination of the Rotational Constant of the Cs_2 $0_g^-(6s + 6p_{3/2})$ State by Trap Loss Spectroscopy. *Opt. Express* **2010**, *18*, 17089–17095.
- (14) Fioretti, A.; Comparat, D.; Drag, C.; Amiot, C.; Dulieu, O.; Masnou-Seeuws, F.; Pillet, P. Photoassociative Spectroscopy of the Cs_2 0_g^- Long-Range State. *Eur. Phys. J. D* **1999**, *5*, 389–403.
- (15) Raab, M.; Weickenmeier, H.; Demtroder, W. The Dissociation Energy of the Cesium Dimer. *Chem. Phys. Lett.* **1982**, *88*, 377–383.
- (16) Weickenmeier, W.; Diemer, U.; Wahl, M.; Raab, M.; Demtröder, W.; Müller, W. Accurate Ground State Potential of Cs_2 up to the Dissociation Limit. *J. Chem. Phys.* **1985**, *82*, 5354–5363.
- (17) Weickenmeier, H.; Diemer, U.; Demtroder, W.; Broyer, M. Hyperfine Interaction between the Singlet and Triplet Ground States of Cs_2 . A Textbook Example of Gerade-Ungerade Symmetry Breaking. *Chem. Phys. Lett.* **1986**, *124*, 470–477.
- (18) Wang, L. R.; Ma, J.; Li, C. Y.; Zhao, J. M.; Xiao, L. T.; Jia, S. T. A High Sensitive Photoassociation Spectroscopy Based on Modulated Ultra-cold Cs Atoms. *Appl. Phys. B: Laser Opt.* **2007**, *89*, 53–57.
- (19) Santos, F. P. D.; Perales, F.; Leonard, J.; Sinatra, A.; Wang, J. M.; Pavone, F. S.; Rasel, E.; Unnikrishnan, C. S.; Leduc, M. Penning Collisions of Laser-Cooled Metastable Helium Atoms. *Eur. Phys. J. D* **2001**, *14*, 15–22.

- (20) Pichler, M.; Chen, H. M.; Stwalley, W. C. Photoassociation Spectroscopy of Ultracold Cs Below the $6P_{3/2}$ Limit. *J. Chem. Phys.* **2004**, *121*, 6779.
- (21) Zhang, Y. C.; Ma, J.; Li, Y. Q.; Wu, J. Z.; Zhang, L. J.; Chen, G.; Wang, L. R.; Zhao, Y. T.; Xiao, L. T.; Jia, S. T. Direct Measurement of Laser-Induced Frequency Shift Rate of Ultracold Cesium Molecules by Analyzing Losses of Trapped Atoms. *Appl. Phys. Lett.* **2012**, *101*, 131114.
- (22) Comparat, D.; Drag, C.; Fioretti, A.; Dulieu, O.; Pillet, P. Photoassociative Spectroscopy and Formation of Cold Molecules in Cold Cesium Vapor: Trap-Loss Spectrum versus Ion Spectrum. *J. Mol. Spectrosc.* **1999**, *195*, 229–235.
- (23) Wu, J. Z.; Ma, J.; Zhang, Y. C.; Li, Y. Q.; Wang, L. R.; Zhao, Y. T.; Chen, G.; Xiao, L. T.; Jia, S. T. High Sensitive Trap Loss Spectroscopic Detection of the Lowest Vibrational Levels of Ultracold Molecules. *Phys. Chem. Chem. Phys.* **2011**, *13*, 18921–18925.
- (24) Bransden, B. H.; Joachain, C. J. *Physics of Atoms and Molecules*; Longman Group UK Limited: Essex, U.K.; 1983.
- (25) Bouloufa, N.; Crubellier, A.; Dulieu, O. Reexamination of the 0_g^- Pure Long-Range State of Cs_2 : Prediction of Missing Levels in the Photoassociation Spectrum. *Phys. Rev. A* **2007**, *75*, 052501.
- (26) Pichler, M.; Stwalley, W. C.; Dulieu, O. Perturbation Effects in Photoassociation Spectra of Ultracold Cs_2 . *J. Phys. B: At. Mol. Opt. Phys.* **2006**, *39*, S981–S992.
- (27) Danzl, J. G.; Haller, E.; Gustavsson, M.; Mark, M. J.; Hart, R.; Bouloufa, N.; Dulieu, O.; Ritsch, H.; Nägerl, H. C. Quantum Gas of Deeply Bound Ground State Molecules. *Science* **2008**, *321*, 1062–1066.